Available online at www.sciencedirect.com
ScienceDirect
Journal of Power Sources 175 (2008) 211–216
JOURNAL OF POWER SOURCES
www.elsevier.com/locate/jpowsour

Short communication

Platinum/carbon nanofiber nanocomposite synthesized by electrophoretic deposition as electrocatalyst for oxygen reduction

Jun-Sheng Zheng, Ming-Xia Wang, Xin-Sheng Zhang *, Yun-Xia Wu, Ping Li, Xing-Gui Zhou, Wei-Kang Yuan

UNILAB, State Key Laboratory of Chemical Engineering, East China University of Science & Technology, Shanghai 200237, China

Received 29 July 2007; received in revised form 14 September 2007; accepted 17 September 2007
Available online 26 September 2007

Abstract

A platinum/carbon nanofiber (Pt/CNF) nanocomposite with a platinum loading of 15 wt% is prepared by a modified electrophoretic deposition (EPD) method, and the as-grown nanocomposite is used as the electrocatalyst for oxygen reduction reaction (ORR). For comparison, a Pt/CNF composite with 40 wt% platinum loading is prepared by chemical reduction. High resolution transmission electron microscope (HRTEM) images show that the size of platinum nanoparticles formed by EPD is about 1 nm, much smaller than those by chemical reduction (about 3–5 nm). Cyclic voltammetric analysis in a nitrogen saturated electrolyte shows that the electrochemical surface area of electrocatalyst by EPD is larger than that by chemical reduction. Moreover, although the electrocatalyst prepared by chemical reduction has a higher electrochemical capacity, it is less active than that prepared by EPD. Analysis of the electrode kinetics using Tafel plot suggests that the electrocatalyst prepared by EPD provides a strong ORR activity. Cyclic voltammetric measurements at different scan rates confirm that the ORR on the nanocomposites prepared by EPD is a diffusion-controlled process. This work demonstrates that the Pt/CNF composites synthesized by EPD are effective for ORR.

Keywords: Carbon nanofiber; Electrophoretic deposition; Oxygen reduction reaction; Electrocatalytic properties

1. Introduction

Direct methanol fuel cell (DMFC) is one of the most promising options for mobile power source because of its high energy conversion efficiency and low pollutant emission [1,2]. Currently, the biggest obstacles to commercial use of the DMFCs are the efficiency and power density. Slow kinetics of the oxygen reduction reaction (ORR) at the cathode of DMFCs is the main problem [3,4]. Correspondingly a large number of investigations have been made to increase the ORR performance by using highly active electrocatalysts. It is well-known that platinum is the best single metal electrocatalyst for oxygen reduction [5,6]. When dispersed as nanoparticles, its shape, size, and interaction with support are the key factors that determine the ORR activity [7], which are manipulated and controlled by selecting proper support materials [8] and following certain synthesis procedures [9].

Carbon black, such as Vulcan XC-72, is most widely used as fuel cell catalyst support because of its good compromise between electronic conductivity and surface area [10–14]. In addition, some new carbon materials with special physicochemical properties, such as ordered porous carbons, graphite fibers, C_{60} clusters and carbon nanotubes (CNTs), have been studied as supports for ORR electrocatalysts. CNTs were shown to have higher ORR activities when used as electrocatalyst support than traditional carbon materials [15–22]. Nevertheless, the CNTs have relative small specific surface area and weak interactions with the supported metals, which restrict further improvement of the ORR activity. These shortcomings can probably be overcome by using other types, e.g. platelet and herringbone, carbon nanofibers (CNFs) as the supports because they have larger surface area and more edge atoms. Particularly,

* Corresponding author. Tel.: +86 21 64253469; fax: +86 21 64253528.
E-mail address: xszhang@ecust.edu.cn (X.-S. Zhang).

0378-7753/$ – see front matter © 2007 Elsevier B.V. All rights reserved.
doi:10.1016/j.jpowsour.2007.09.058

the platelet type CNFs, which have a higher ratio of edge atoms to basal atoms than other types of CNFs, are easier to adjust the metal deposition. Published results show that electrocatalysts with platelet CNFs as support exhibit higher ORR activity than those with other supporting materials. For example, Bessel et al. [23] used Pt/CNFs and Pt/(Vulcan XC-72) as the electrocatalysts for DMFCs, and found that 5 wt% platinum supported on the platelet CNFs was as active as 25 wt% platinum supported on Vulcan XC-72. Similarly, we found that palladium particles supported on platelet type CNFs had higher ORR activities than those on fish-bone CNFs or activated carbons [24].

The platinum loading processes also have distinct influences on metal dispersion and metal-support interaction. Several different metal loading processes, such as chemical reduction [25], electrodeposition [26], physical evaporation [27], etc. have been proposed and investigated. Platinum nanoparticles were supported on Vulcan XC-72 through the reduction of chloroplatinic acid with formic acid [25]. By chemical reduction in H_2 at 580 °C, platinum particles with very narrow size distribution were grown in CNT membranes [28]. But the chemical reduction of the metal precursors does not provide adequate control of particles shape and size. In addition, chemical reduction is time-consuming.

Recently, electrodeposition has been employed as an effective means of metal deposition on carbon materials. This method is simple compared to chemical reduction and the metal loading can easily be controlled. Moreover, the prepared catalysts are free from the contamination of excessive reducers, protecting surfactants, etc. Tang et al. [29] deposited platinum on glassy carbon (GC) by cyclic voltammetry and showed that the platinum particles had small particle size and good electrocatalytic activity. Chen and co-workers [26] reported that platinum nanoparticles could be uniformly dispersed on the surface of CNTs by potentiostatic method using H_2PtCl_6 aqueous solution at the potential of −0.25 V (versus SCE). But there still remains a challenge for the preparation of narrow sized metal nanoparticles over carbon materials by electrodeposition. Platinum nanoparticles prepared by electrodeposition are mostly larger than 50 nm. In addition, it is not easy to estimate metal loadings from the deposition charge.

In a recent paper, electrophoretic deposition (EPD) has been proven to be a direct and efficient approach to prepare nanoparticles or nanocomposites [30]. The conventional EPD is essentially a two-step process, which involves electrophoresis and deposition. First, the support and the metal particles suspended in liquid are forced to move towards the electrode by electric field. Second, the particles collect at the electrode and form a coherent deposit [31].

In this paper, we demonstrate the possibility of anchoring platinum nanoparticles on the surface of CNFs by a modified EPD process. In traditional EPD, the support is first charged and suspended in the solution and then move to the carrier by electric field force. Since the relatively heavier of support, the EPD potential is evident high (mostly higher than 50 V). To avoid the troublesome electrophoresis of support, CNFs were directly coated on the surface of a GC electrode by using Nafion as a binder. The purpose of the present work is to demonstrate the possibility of synthesize of platinum nanoparticles on the surface of CNFs by the mentioned EPD and to compare the oxygen reduction behavior of nanoparticles by EPD with those prepared by chemical reduction.

2. Experimental

2.1. Preparation of CNFs and electrocatalyst

CNFs were synthesized by decomposition of CO on iron catalyst in a fixed-bed quartz reactor by catalytic chemical vapor deposition (CCVD). In brief, 1 g of the catalyst precursor containing iron was placed in a horizontal quartz tube reactor of 40 mm i.d. and 500 mm length, and was then reduced in a flow of H_2 (40 ml min^{-1}) and Ar (120 ml min^{-1}) at 600 °C for 3 h. At the same temperature, CNFs started to grow when the gas flow was changed to a mixture of CO (40 ml min^{-1}) and H_2 (20 ml min^{-1}) and about 10 g CNFs were obtained in 16 h. The details of the synthesis procedure were also described in the Ref. [32].

Electrocatalyst with a platinum content of 40 wt% (Pt/CNFs-CR) was prepared by chemical reduction, and the procedure was described in [25]. Electrocatalyst with a platinum content of 15 wt% (Pt/CNFs-EPD) was prepared by EPD according to the following procedure. The platinum colloid solution was first prepared by using H_2PtCl_6 as the precursor, the details of which is referred to [32]. Then, the CNFs were coated on the surface of a 3-mm diameter GC electrode, which is prepared by a procedure described below. Finally, the CNF modified electrode was immerged into the colloid solution, and the platinum nanoparticles were anchored to the CNFs by EPD at potential of 0.10 V versus the open-current potential.

2.2. Preparation and modification of electrode

Electrocatalyst or CNF powder was dispersed ultrasonically in a 0.5 wt% Nafion solution to obtain a homogenous black suspension with a concentration of 5 mg ml^{-1}. A 10 μl solution was pipetted onto the surface of a 3-mm diameter GC electrode. Before surface modification, the GC electrode was polished with 0.3 and 0.05 μm alumina slurries, washed by acetone, ethanol and water, and then subjected to ultrasonic agitation for 5 min in ultrapure water. The surface modified GC electrode was dried at room temperature and in ambient air for 1 h and was washed with ultrapure water before use.

2.3. Electrocatalyst characterization

The morphologies of the catalysts were characterized by high resolution transmission electron microscope (HRTEM, JEOL TEM 2010). The operating voltage on the microscope was 200 keV. To obtain HRTEM images, the as-synthesized platinum-modified CNF powders were dispersed in ethanol solution under ultrasonic agitation for 1 min and then deposited on a copper–carbon grid. Electrochemical measurements were performed on an Autolab Potentiostat 30 electrochemical

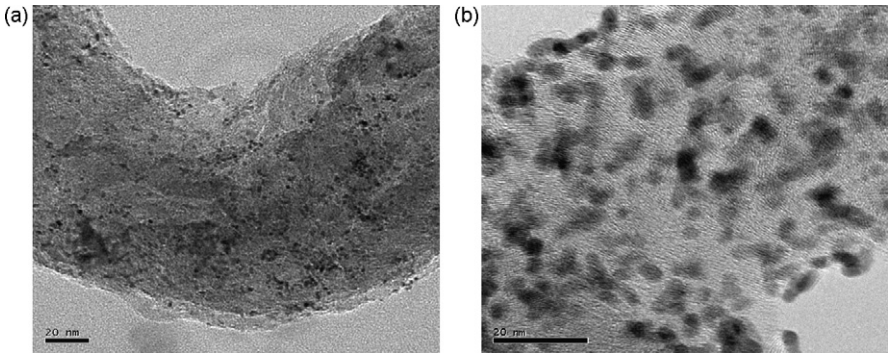

Fig. 1. Typical HRTEM images of Pt/CNFs-EPD (a) and Pt/CNFs-CR (b). The platinum content of Pt/CNFs-EPD and Pt/CNFs-CR is 15 wt% and 40 wt%, respectively.

workstation (Eco Chemie B.V., the Netherlands) in a 0.5 M $HClO_4$ solution. The working electrode was GC coated with different electrocatalysts. A saturated calomel reference electrode (SCE) was used as reference electrode for all electrochemical measurements and all the potentials were reported versus this reference electrode. A platinum clump was used as the counter electrode. Fresh electrolyte solution was used every time to make the measurement reproducible and reliable.

3. Results and discussion

3.1. Microstructures of CNFs decorated with platinum nanoparticles

Fig. 1 shows the HRTEM images of the isolated Pt/CNFs-EPD and Pt/CNFs-CR. The CNFs have a diameter of about 100 nm, and the graphene layers of the CNFs are vertical to the fiber axis. Fig. 1 also shows that the platinum nanoparticles on the CNFs have a very uniform size distribution. The platinum nanoparticles anchored by EPD is about 1 nm, much smaller than those prepared by chemical reduction, which are about 3–5 nm.

The difference in platinum nanoparticle sizes was caused by the different synthesis processes. In chemical reduction, the platinum ions were located on the CNF surface, which was then reduced to metal particles. These nanoparticles may coalescence in the post-treatment process, such as filtration and drying, to form large particles. In EPD, platinum colloids were first charged and deposited onto CNF surface by electric force. Because the nanoparticles were charged before deposition, coalescence was less possible to happen because of electrostatic repulsion. This is the main reason for the smaller particles prepared by EPD.

Cyclic voltammograms for Pt/CNFs-EPD and Pt/CNFs-CR using a nitrogen saturated 0.5 M $HClO_4$ electrolyte, in the potential range of 1.25 to −0.25 V and with a scan rate of 10 mV s^{-1}, are presented in Fig. 2. A reduction peak centered around 0.50 and 0.30 V can be observed during the negative-going potential sweeps of Pt/CNFs-EPD and Pt/CNFs-CR, respectively, which can be attributed to the platinum oxide reduction peak [33]. This is a further evidence of the presence of platinum on the electrodes.

3.2. Electrochemical surface area

From Fig. 2, one can observe the hydrogen absorption/desorption peaks for Pt/CNFs-EPD and Pt/CNFs-CR. The charge exchange during eletroadsorption of H atom on platinum is obtained by integrating the charge between −0.25 and 0.00 V [34]. Then the electrochemical surface area of electrocatalyst, i.e. S_{EL}, is calculated from

$$S_{EL} = \frac{Q_H}{Q_{Href}} \quad (1)$$

where Q_H is the charge exchange during eletroadsorption of H atom on platinum and Q_{Href} is the charge absorbed on the surface of platinum (0.21 mC cm^{-2} [35]).

The calculated charge exchange, electrochemical surface area, and specific surface area of different electrocatalysts are listed in Table 1. Although Pt/CNFs-EPD has a lower platinum

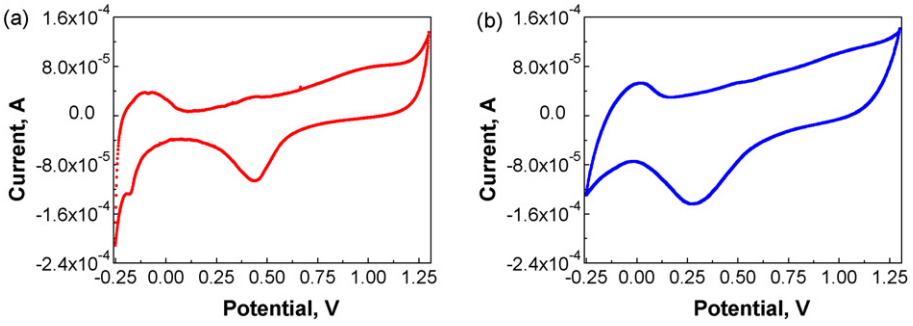

Fig. 2. Cyclic voltammograms in a N_2 saturated 0.5 M $HClO_4$ solution for Pt/CNFs-EPD (a) and Pt/CNFs-CR (b). The platinum content of Pt/CNFs-EPD and Pt/CNFs-CR is 15 wt% and 40 wt%, respectively.

Table 1
Electrochemical surface area of different electrocatalyst samples determined by H_2 electroadsorption

Sample	m(Cat) (μg)	m(Pt) (μg)	Q_H/mC	S_{EL} (cm^2)	A_{EL} ($m^2\ g^{-1}$)
Pt/CNFs-CR	50.0	20.0	0.55	2.62	13.10
Pt/CNFs-EPD	58.5	8.77	0.67	3.19	36.37

Q_H: charge exchange during electroadsorption of H atom on platinum; S_{EL}: electrochemical surface area obtained electrochemically according to Eq. (1); A_{EL}: specific surface area (=S_{EL}/m(Pt)).

loading, its electrochemical surface area (3.19 cm^2) is larger than that of Pt/CNFs-CR (2.62 cm^2) and its specific surface area (36.37 $m^2\ g^{-1}$) is almost three times larger than that of Pt/CNFs-CR (13.10 $m^2\ g^{-1}$). The high electrochemical surface area and specific surface area of Pt/CNFs-EPD is advantages for its application in DMFCs.

3.3. Electrocatalytic activity of ORR

3.3.1. ORR onset reduction potential and current

Fig. 3 depicts the results of cyclic voltammetric study of the two electrocatalysts at the scan rate of 10 mV s^{-1} in a 0.5 M $HClO_4$ electrolyte saturated by N_2 and O_2. The experiments were determined according to the following procedures. The electrolyte was first bubbled with nitrogen for 30 min to purge the oxygen, and the current–potential was recorded in the presence of nitrogen. Then, the electrolyte was saturated with oxygen and the current–potential curve was recorded, too. From curve 1 in Fig. 3, we can find that Pt/CNFs-CR exhibits a background current larger than Pt/CNFs-EPD. This reveals that the electrochemical capacity of Pt/CNFs-EPD is smaller than that of Pt/CNFs-CR, and this can be attributed to the smaller platinum loading of the Pt/CNFs-EPD.

The ORR onset reduction potential of Pt/CNFs-EPD is 0.75 V, more positive than that of Pt/CNFs-CR (0.65 V). It is believed that the different ORR onset reduction potentials are caused by the differences in the surface activation of various catalysts [7,22], and the more positive ORR onset reduction potential of Pt/CNFs-EPD reveals that Pt/CNFs-EPD is more active than Pt/CNFs-CR. The reasons for the different ORR activities are twofold. On one hand, the higher ORR activity of Pt/CNFs-EPD can be attributed to the smaller platinum particle size. Moreover, since Pt/CNFs-EPD are synthesized in platinum colloid by EPD, platinum nanoparticles may be orientated on the energetic edge atoms, and this may promote the metal-support interaction and may be the other reason for the higher ORR activity of Pt/CNFs-EPD.

Table 2
ORR current of different electrocatalyst samples at the potential of 0.6 V

Sample	Current (μA)	Mass current density A $(mg\ Pt)^{-1}$	Specific current density ($A\ cm^{-2}$)
Pt/CNFs-CR	4.09	2.05×10^{-04}	1.56×10^{-03}
Pt/CNFs-EPD	20.20	2.30×10^{-03}	6.33×10^{-03}

Mass current density: current/m(Pt); specific current density: current/S_{EL}.

Table 2 lists the oxygen reduction current at a potential of 0.60 V versus SCE (in kinetically controlled region) with a scan rate of 10 mV s^{-1}. The mass current density of Pt/CNFs-EPD (2.30×10^{-03} A $(mg\ Pt)^{-1}$) is found to be about 10 times larger than that of Pt/CNFs-CR (2.05×10^{-04} A $(mg\ Pt)^{-1}$). One reason for the differences in the mass current densities of the two electrocatalysts is the smaller platinum size on Pt/CNFs-EPD. The other reason may be caused by the relatively higher activity of Pt/CNFs-EPD compared with Pt/CNFs-CR. At the kinetically controlled region, the current increases when the potential decreases for the increase in the degree of catalyst surface activation for a reduction reaction. Pt/CNFs-CR is less active than Pt/CNFs-EPD, then the degree of surface activation of Pt/CNFs-CR is lower than that of Pt/CNFs-EPD at the same potential (0.60 V versus SCE), and this is another reason for the lower ORR current density of Pt/CNFs-CR.

Shown in Fig. 4 is the plot of log i versus potential for fresh Pt/CNFs-EPD and Pt/CNFs-CR. The apparent exchange current densities were obtained by extrapolating the linear region to zero overpotential and are listed in Table 3. A commercially available Pt/C electrocatalyst with a platinum content of 20 wt% and a Pt/CNTs with a platinum content of 25 wt% were selected as references and their apparent exchange current density are also presented in Table 3. The apparent exchange current density of Pt/CNFs-EPD and Pt/CNFs-CR is 8.91×10^{-5} A cm^{-2} and 1.28×10^{-4} A cm^{-2}, respectively, much higher than that of Pt/CNTs [7] and commercial Pt/C [36]. The differences between our electrocatalysts and the electrocatalysts reported by others may be caused by the different loading of plat-

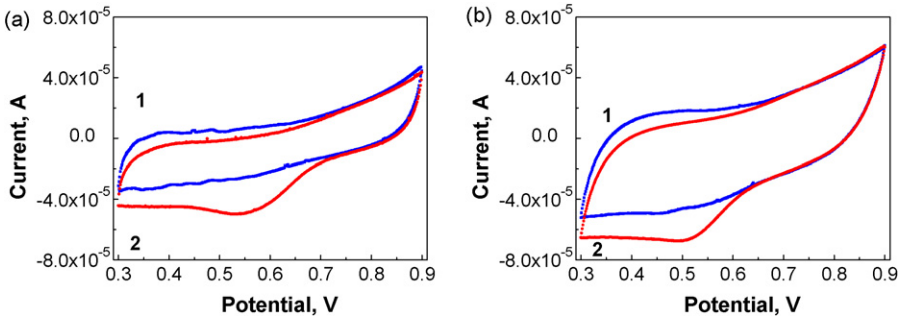

Fig. 3. Cyclic voltammetric analysis of different electrodes in a 0.5 M $HClO_4$ solution saturated by nitrogen (1) and oxygen (2) at scan rate of 10 mV s^{-1}: (a) Pt/CNFs-EPD and (b) Pt/CNFs-CR. The platinum content of Pt/CNFs-EPD and Pt/CNFs-CR is 15 wt% and 40 wt%, respectively.

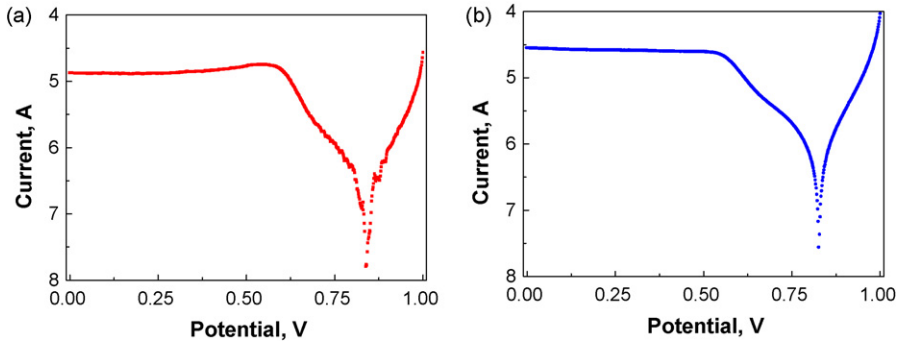

Fig. 4. Tafel polarization curve for Pt/CNFs-EPD (a) and Pt/CNFs-CR (b) in a 0.5 M $HClO_4$ solution saturated by oxygen at 1 mV s^{-1}. The platinum content of Pt/CNFs-EPD and Pt/CNFs-CR is 15 wt% and 40 wt%, respectively.

Table 3
Apparent exchange current density of the different electrocatalysts

Sample	Apparent exchange current density (A cm^{-2})	References
Pt/CNFs-CR	8.91×10^{-5}	This work
Pt/CNFs-EPD	1.28×10^{-4}	This work
Pt/CNTs[a]	8.90×10^{-7}	[7]
Pt/C[b]	1.09×10^{-7}	[36]

[a] The platinum content of Pt/CNTs is 25 wt%.
[b] The commercial catalyst corresponds to Pt on carbon (20% Pt/C) with loadings of 0.4 mg cm^{-2} on 125 mm^2 Nafion Dupont membranes.

inum, different support, or different methods of preparing electrocatalysts.

3.3.2. ORR peak potential and reaction process

For ORR, increasing the potential will increase the surface activity and accordingly increase the current. But when the process is controlled by diffusion, the reduction current will not increase further because of the shortage of the reactant on the electrode surface. Therefore if the reactant is deficient on the electrocatalyst surface, an ORR peak will appear [24]. The oxygen reduction peaks of Pt/CNFs-EPD and Pt/CNFs-CR were around 0.55 and 0.50 V, respectively, as shown in Fig. 3. Since the oxygen concentrations remains unchanged for all the experiments, the ORR peak potential is determined by the relative rate of diffusion and surface reaction. The supports of the Pt/CNFs-EPD and Pt/CNFs-CR are the same, and then the diffusion processes on the two electrocatalysts are similar. So, the different ORR peak potentials can reflect the differences in ORR activities. The more positive ORR peak potential of Pt/CNFs-EPD than that of Pt/CNFs-CR proves the higher ORR activity of Pt/CNFs-EPD.

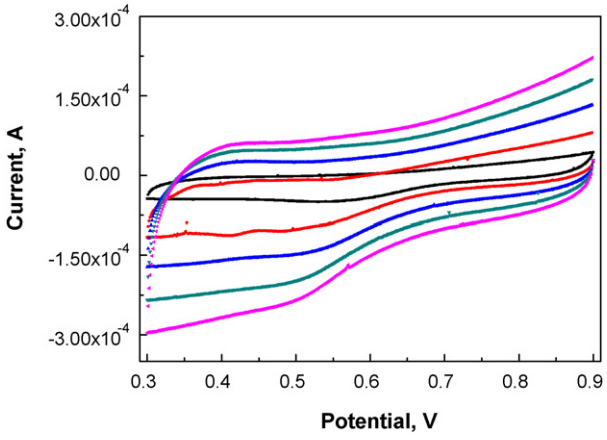

Fig. 5. Cyclic voltammetric analysis of oxygen reduction at Pt/CNFs-EPD with different scan rates in an oxygen saturated 0.5 M $HClO_4$ solution. The scan rates are 10, 25, 50, 75, and 100 mV s^{-1} from inside to outside, respectively.

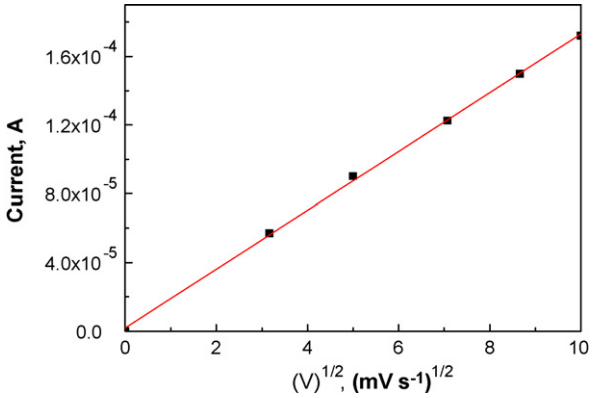

Fig. 6. Linear plot of ORR peak currents as a function of the square root of scan rates (scan rates: 10, 25, 50, 75 and 100 mV s^{-1}) of Pt/CNFs-EPD.

Shown in Fig. 5 is the cyclic voltammogram of Pt/CNFs-EPD electrode at different scan rates in an oxygen saturated 0.5 M $HClO_4$ electrolyte. The ORR peak currents as a function of the square root of the scan rates of Pt/CNFs-EPD are plotted in Fig. 6, which indicates that ORR peak current varies linearly with the square root of the scan rates and passes through the origin of coordinates. This fact confirms that ORR on Pt/CNFs-EPD is controlled by diffusion. Similar results were observed on a GC electrode modified by Pt/CNTs [7] and Pd/CNTs [15].

4. Conclusion

A platinum/carbon nanofiber (Pt/CNF) composite with a platinum loading of 15 wt% and an averaged platinum particle size of 1 nm is prepared and its performance compared with a composite prepared by chemical reduction and with a metal loading of 40 wt%. Although the composite prepared by EPD has a much

smaller metal loading, it has a specific surface area three times higher than that prepared by chemical reduction and exhibits a higher ORR onset reduction potential, ORR peak potential and larger ORR current. All this can be attributed to the smaller particles formed by EPD and possibly by different metal-support interaction. Tafel plot suggests that electrocatalyst synthesized by EPD has a strong ORR activity and cyclic voltammetric analysis at different scan rates reveals that ORR on electrocatalyst prepared by EPD is controlled by diffusion. The results presented in this paper indicate that EPD is efficient for the preparation of electrocatalysts for ORR.

Acknowledgements

The authors acknowledge the support from the Shanghai Key Laboratory of Green Chemistry and Chemical Processes (East China Normal University), the Raising State Key Laboratory of Green Chemistry Synthesis Technology (Zhejiang University of Technology), the NSFC/PetroChina major project (No. 20490200), and the special funding for the state key laboratories sponsored by the Science and Technology Committee of Shanghai Municipality, China (No. 036505010).

References

[1] A.S. Arico, S. Srinivasan, V. Antonucci, Fuel Cells 1 (2001) 133–136.
[2] K.Y. Chan, J. Ding, J.W. Ren, S.A. Cheng, K.Y. Tsang, J. Mater. Chem. 14 (2004) 505–516.
[3] M.S. Loffler, B. Gross, H. Natter, R. Hempelmann, T. Krajewski, J. Divisek, Phys. Chem. Chem. Phys. 3 (2001) 333–338.
[4] A. Lima, C. Coutanceau, J.M. Leger, C. Lamy, J. Appl. Electrochem. 31 (2001) 379–386.
[5] S. Katsuaki, U. Kohei, K. Hideaki, N. Yoshinobu, J. Electroanal. Chem. 256 (1988) 481–487.
[6] M. Watanabe, S. Saegusa, P. Stonelhart, J. Electroanal. Chem. 271 (1989) 213–217.
[7] Y. Lin, X. Cui, C. Chen, C. Wai, J. Phys. Chem. B 109 (2005) 14410–14415.
[8] Z. Liu, X.Y. Ling, X. Su, J.Y. Lee, J. Phys. Chem. B 108 (2004) 8234–8240.
[9] V. Lordi, N. Yao, J. Wei, Chem. Mater. 13 (2001) 733–735.
[10] Z. Liu, X.Y. Ing, X. Su, J.Y. Lee, J. Phys. Chem. B 108 (2004) 8234–8240.
[11] Q. Lu, B. Yang, L. Zhuang, J. Lu, J. Phys. Chem. B 109 (2005) 1715–1722.
[12] Z.L. Liu, L.M. Gan, L. Hong, W.X. Chen, J.Y. Lee, J. Power Sources 139 (2005) 73–78.
[13] J.T. Moore, J.D. Corn, D. Chu, R. Jiang, D.L. Boxall, E.A. Kenik, C.M. Lukehart, Chem. Mater. 15 (2003) 3320–3325.
[14] W.H. Lizcano-Valbuena, D.C. Azevedo, E.R. Gonzalez, Electrochim. Acta 49 (2004) 1289–1295.
[15] Y. Lin, X. Cui, X. Ye, Electrochem. Commun. 7 (2005) 267–274.
[16] P.J. Britto, K.S.V. Santhanam, A. Rubio, J.A. Alonso, P.M. Ajayan, Adv. Mater. 11 (1999) 154–157.
[17] J. Wang, M. Musameh, Y. Lin, J. Am. Chem. Soc. 125 (2003) 2408–2409.
[18] N. Rajalakshmi, H. Ryu, M.M. Shaijumon, S. Ramaprabhu, J. Power Sources 140 (2005) 250–257.
[19] X. Wang, W.Z. Li, Z.W. Chen, M. Waje, Y.S. Yan, J. Power Sources 158 (2006) 154–159.
[20] Y. Lin, F. Lu, J. Wang, Electroanalysis 16 (2004) 145–149.
[21] M. Musameh, J. Wang, A. Merkoci, Y. Lin, Electrochem. Commun. 4 (2002) 743.
[22] Y.Y. Shao, G.P. Yin, J.J. Wang, Y.Z. Gao, P.F. Shi, J. Power Sources 161 (2006) 47–53.
[23] C.A. Bessel, K. Laubernds, N.M. Rodriguez, R. Baker, K. Terry, J. Phys. Chem. B 105 (2001) 1115–1118.
[24] J.S. Zheng, X.S. Zhang, P. Li, J. Zhu, X.G. Zhou, W.K. Yuan, Electrochem. Commun. 9 (2007) 895–900.
[25] T.J. Zhao, Ph.D. Thesis, East China University of Science and Technology, 2004.
[26] Z. He, J. Chen, D. Liu, H. Zhou, Y. Kuang, Diam. Relat. Mater. 13 (2004) 1764–1769.
[27] Y. Zhang, H. Dai, J. Appl. Phys. Lett. 77 (2000) 3015–3017.
[28] G.S. Che, B.B. Lakshmi, E.R. Fisher, C.R. Martin, Nature 393 (1998) 346–349.
[29] H. Tang, J.H. Chen, Z.P. Huang, D.Z. Wang, Z.F. Ren, L.H. Nie, Y.F. Kuang, S.Z. Yao, Carbon 42 (2004) 191–197.
[30] A.R. Boccaccine, J. Cho, J.A. Roether, B.J.C. Thomas, E.J. Miny, M.S.P. Shaffer, Carbon 44 (2006) 3149–3160.
[31] O. Van der Biest, L.J. Vandeperre, Annu. Rev. Mater. Sci. 298 (1999) 327–352.
[32] Z.J. Sui, Ph.D. Thesis, East China University of Science and Technology, 2005.
[33] J. Chen, M. Wang, B. Liu, Z. Fan, K. Cui, Y. Kuang, J. Phys. Chem. B 110 (2006) 11775–11779.
[34] J. Zhang, K. Sasaki, E. Sutter, R.R. Adzic, Science 315 (2007) 220–222.
[35] T.R. Ralph, G.A. Hards, J.E. Keating, S.A. Campbell, D.P. Wilkinson, M. Davis, J. St-Pierre, M.C. Johnson, J. Electrochem. Soc. 144 (1997) 3845–3857.
[36] T. Vargas, R. Varma, in: R. Varma, J.R. Selman (Eds.), Techniques for Characterization of Electrodes and Electrochemical Processes, Wiley, Chichester, 1991, p. 717.